

## Recovering molecular orientation from convoluted orbitals

Andrew J. Lakin, Cristina Chiutu, Adam M. Sweetman, Philip Moriarty, and Janette L. Dunn\*

*School of Physics and Astronomy, University of Nottingham, Nottingham, NG7 2RD, United Kingdom*

(Received 16 May 2013; published 31 July 2013)

Scanning probe microscopy lets us “see” atoms and molecules with unprecedented detail, particularly when the resolution is enhanced by functionalizing the tip of the microscope through deliberate adsorption of atomic or molecular species. However, interpreting the resultant images is often far from trivial as they contain features of both the tip and the sample. Here, a computationally simple theoretical approach is presented that allows the orientations of the tip and sample molecules to be determined from a single scanning tunneling microscopy (STM) image, which in turn reveals information on the bonding interaction between the molecules and the tip and surface. We use the approach to deconvolve the experimental STM images arising from the interaction between a  $C_{60}$ -functionalized tip and a  $C_{60}$  molecule adsorbed on a  $Si(111)-(7 \times 7)$  surface. The results provide experimental verification of the surface orientations postulated theoretically by Ruruli *et al.* [*Phys. Rev. B* **81**, 075419 (2010)].

DOI: [10.1103/PhysRevB.88.035447](https://doi.org/10.1103/PhysRevB.88.035447)

PACS number(s): 61.48.–c, 68.37.Ef, 68.43.Fg, 81.05.ub

### I. INTRODUCTION

Recent advances in scanning probe microscopy have allowed images of individual organic molecules to be obtained at unprecedented resolution, where, as illustrated through the pioneering work undertaken by Gross and co-workers,<sup>1</sup> it is often the functionalization of the tip, through deliberate adsorption of a specific atom or molecule, that allows this high resolution to be obtained.<sup>2</sup> This has directed much research into associated techniques, with work ranging from, among others, the imaging of ferromagnetic domains,<sup>3</sup> molecular identification,<sup>4</sup> and the analysis of intermolecular forces.<sup>5,6</sup> The common feature of all of this work is the reliance on the careful manipulation and control of the tip state, and an understanding of the interaction between the tip and sample.

While much of the work undertaken so far has focused on the force interaction observed during atomic force microscopy (AFM), there is still considerable benefit in interpreting the scanning tunneling microscopy (STM) images obtained from a functionalized tip, as initially shown in the reverse imaging experiments of Herz *et al.*<sup>7</sup> where the effect of the tip state on STM images of a  $Si(111)-(7 \times 7)$  surface was investigated. In addition, the work undertaken by Gross *et al.*<sup>8</sup> examined the effects of a tip formed from a combination of  $p_x$  and  $p_y$  orbitals, while Schull and co-workers used STM to determine the molecular orientation of a tip-adsorbed  $C_{60}$  from the interaction with both Au and Cu clusters.<sup>9,10</sup>

Interpreting the convoluted STM images obtained from a nonsimple tip is a long-standing problem. Since the work by Herz *et al.*,<sup>7</sup> much work has been undertaken to accurately interpret the tip structure directly from STM images. This is exemplified by a series of works from Chaika and co-workers,<sup>11–14</sup> looking at the accurate description of the tip termination through the interaction with a known surface structure. The importance of the tip termination to the obtained STM images is also shown in more general terms, in the work undertaken by Loos,<sup>15</sup> Hagelaar *et al.*,<sup>16</sup> and Gottlieb and Wesoloski.<sup>17</sup> As any STM image will be formed from contributions from both tip and sample, it is clear that understanding the tip structure is essential in interpreting the resultant image.

In general, STM imaging provides a map of the local density of states within an energy window defined by the tip-sample bias (although important exceptions do exist<sup>18</sup>) which does not usually correlate with the positions of atoms within a molecule. It is therefore not usually possible to obtain the atomic positions directly from an image to elucidate the molecular orientation. Hence, considerable theoretical input is needed. Currently, this theoretical analysis is almost exclusively undertaken utilizing density functional theory (DFT), which, while of significant use in a large number of cases, is often time consuming due to its considerable computational expense. In more complicated systems such as those often present when a functionalized tip is considered, the computational expense is so great as to limit the effectiveness of DFT as an investigative tool, so for these cases development of an alternative method is essential. This is exemplified by previous work using a  $C_{60}$ -functionalized tip. Švec *et al.*<sup>19</sup> investigated a  $C_{60}$  monolayer adsorbed on graphene, and Hauptmann *et al.*<sup>20</sup> looked at a  $C_{60}$  monolayer present on a  $Cu(111)$  surface. In the former, the extensive DFT calculations required did not allow for the incorporation of the graphene substrate, and in the latter an alternative to DFT was used to interpret the experimental images in the form of a two-dimensional Gaussian approximation for the orbitals of the two molecules that does not incorporate the effects of either the interaction between the surface-adsorbed molecule and the underlying Cu substrate, or that between the tip-adsorbed molecule and the probe. It also only allows the interaction with the nearest faces to be analyzed, and as such can only be considered a low-level approximation (as will be shown here).

The accurate determination of the molecular orientation of both tip- and surface-adsorbed molecule is critical when examining orientationally dependent properties. With the increasing interest in molecular electronics and molecular self-assembly, the understanding of such properties requires a suitable theoretical technique. In this work, we will present a computationally simple approach that allows the orientations of both molecules to be determined, while also considering both tip and substrate interactions. This broadly applicable method will be used to analyze experimental images obtained

when isolated  $C_{60}$  molecules adsorbed on a Si(111)-(7 × 7) surface are imaged using a  $C_{60}$ -functionalized tip. The molecular orientation of both  $C_{60}$  molecules will be found from a single STM image, as well as determining the molecular orbitals (MOs) involved in the tunneling process. We will show that the orientations found confirm predictions of the bonding with the surface made in theoretical work undertaken by Rurali *et al.*<sup>21</sup> using a tight-binding mechanism.

## II. THEORETICAL TECHNIQUE

The tunneling current observed during STM is related to the MOs of both the STM tip and the sample being probed.<sup>22</sup> In general, this tunneling current can be determined using Chen's derivative rule.<sup>23</sup> For the interaction between an orbital with quantum number  $l$  of one species, and a second orbital  $\psi$  of the other, the observed current is found to be proportional to some linear combination of the square of the  $l$ th-order derivatives of  $\psi$ . For  $l = 0$ , where the interaction is with an  $s$ -type orbital, the well-known Tersoff-Hamann approximation<sup>24</sup> is produced where  $I \propto \psi^2$ .

The derivative rule is derived through the properties of the integral associated with Bardeen's matrix element,<sup>22,23</sup> with its use negating the requirement for these time-consuming integrals to be calculated, as would usually be the case for tip-sample convolutions. Instead, a function, that shall be termed the effective current  $I'$ , is found that is proportional to the true current and comprises solely of easily calculated derivatives. For a functionalized tip where a molecule is adsorbed on the probe, expressing the MOs in the form of a linear combination of atomic orbitals (LCAO) allows the interactions between individual sample and tip orbitals to be treated independently, and as such  $I'$  consists of a simple sum over all interacting orbitals. Expressing the MOs in this way requires the use of some LCAO method. As  $I'$  is proportional to the true current, no predictive current values can be found, but the absolute energy of the MOs is unimportant (as long as the ordering of the MOs is correct). As such, computationally simple methods such as the extended Hückel approach, or in certain cases, normal Hückel molecular orbital theory, are ideal.

For molecules where degeneracies exist in the MOs, the interaction between either the tip-adsorbed molecule and the STM probe or the surface-adsorbed molecule and the underlying substrate, is expected to, at least in part, remove these degeneracies. Previously, attempts have been made to model the effects of this bonding by introducing a uniaxial molecular distortion into DFT calculations,<sup>25</sup> and also by looking at the symmetry reduction of the molecule alongside Hückel calculations.<sup>26</sup> In this work, a slightly different method is presented, similar to that used within a tight-binding simulation by Menon *et al.*,<sup>27</sup> where the interaction is modeled using a unidirectional exponentially decaying energy function. Unlike the work by Dunn *et al.*<sup>26</sup> and Pascual *et al.*,<sup>25</sup> where the effect of the bonding mechanism on the atomic structure is considered, here it is the energy change of each of the orbitals introduced through this distortion that is used to model the interaction. A simple diagonal Hamiltonian acting on the complete orbital basis is constructed that represents the change in energy of each orbital at the appropriate diagonal element. For the calculations shown here, the energy function is chosen

to decay with a  $\frac{1}{r^6}$  relationship (to match a van der Waals style interaction), perpendicular to a homogeneous plane situated 0.55 nm from the molecule. However, as the exact energy change is unimportant, the form of the energy function is not critical as long as there is sufficient decay as the distance from the surface increases. In spite of this somewhat simplistic approach to the bonding mechanism, excellent agreement is found with both previous theory and experimental data for the cases examined.

In the case investigated here, where a  $C_{60}$ -functionalized tip images a  $C_{60}$  surface-adsorbed molecule, it is possible to use Hückel molecular orbital theory to obtain the MOs of the molecules in terms of a linear combination of radial  $p$  orbitals.<sup>28</sup> For more general cases, the extended Hückel method can be used. However, standard Hückel theory has been shown previously to produce theoretical STM images of  $C_{60}$  molecules that exhibit excellent agreement with both DFT and experiment.<sup>6,26,29,30</sup>

With the surface-adsorbed molecule centered at a point  $R_0$  with respect to the center of the tip-adsorbed molecule, the complete contribution to the effective current from two interacting MOs can be formed using the derivative rule. As the MOs are linear combinations, each  $p$  orbital associated with the sample molecule can be taken separately, giving the effective current as

$$I'(R_0) = \sum_j^{60} \left( c_j \frac{\partial \psi^T(r_j)}{\partial i} \right)^2, \quad (1)$$

where  $c_j$  is the coefficient of the  $j$ th  $p$  orbital of the sample molecule as determined by the sample MO, with the  $p$  orbital pointing in the  $i$  direction.  $\psi^T(r_j)$  is the MO of the tip-adsorbed molecule, evaluated at the  $j$ th atomic center  $r_j$ , with  $r_j$  defined relative to  $R_0$ . Similarly, the tip-adsorbed molecule can be subdivided into individual  $p$ -orbital contributions to give

$$I'(R_0) = \sum_j^{60} \sum_k^{60} \left( c_j c_k \frac{\partial p_k^T(r_j)}{\partial i} \right)^2, \quad (2)$$

where  $c_k$  is the coefficient of the  $k$ th  $p$  orbital of the tip-adsorbed molecule  $p_k^T$ . Each expression within the sum is then evaluated at the point  $r_j$ .

It is assumed throughout that the energy shift introduced by the bonding interaction is sufficient to allow each MO to be imaged independently during STM. However, there are certain molecular orientations where degeneracies remain, and for these cases the contribution from each MO is simply summed. The choice whether to differentiate the MO of the tip or sample molecule is arbitrary. However, as the interaction between the tip and the adatoms of the Si surface will also be considered (as will be shown), the tip molecule is chosen for this work.

Due to the exponential nature of the atomic orbital functions, only the orbitals associated with closely spaced atoms will provide a significant contribution to the current. For the simulations shown here, the interaction between the 10 nearest atoms (i.e., 100 interactions) at a given point have been considered, although, for investigative purposes little error is introduced by considering only the nearest six interacting atoms (i.e., 36 interactions) which further reduces the computational time. A theoretical raster scan is then

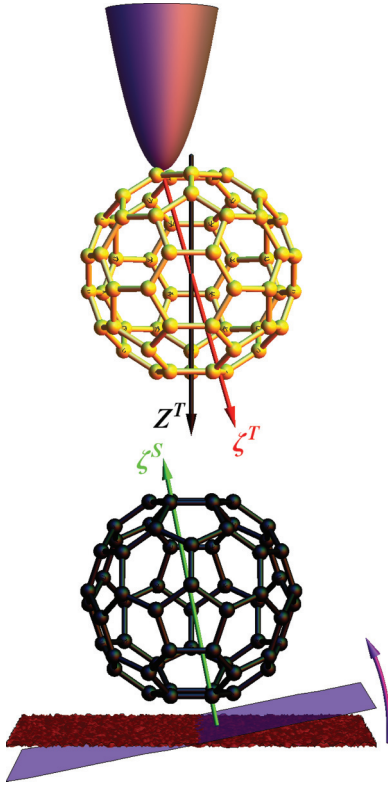


FIG. 1. (Color online) Graphical representation of the system under consideration.  $\zeta^T$  and  $\zeta^S$  represent the direction in which the external interaction is incorporated for the tip and surface molecules, respectively, while  $Z^T$  represents the  $z$  direction of the scan.

undertaken as described by Chiu *et al.*<sup>6</sup> to model the constant current STM mode of operation (a discussion on the link between the theoretical interpretation of constant current STM and the constant average current dSTM can also be found in this reference). It should be noted that the approximation used in taking only the closest atoms differs from that undertaken by Hauptmann *et al.*<sup>20</sup> where the *uppermost* atoms were considered, as here it is the *nearest* atoms at any given tip position that are taken to contribute.

Each molecule has a number of parameters that can be altered (a selection is shown in Fig. 1), with each having a significant effect on the images formed. The relative molecular orientations of both molecules are varied via three rotation angles. Initially, each molecule is defined with  $C_2$  symmetry axes (through the center of a double bond) through each Cartesian axis, with the  $y$  axis through a vertical double bond, and the  $x$  axis through a horizontal double bond. The orientation of the tip-adsorbed molecule is then varied by applying the rotations

$$R_z(\kappa)R_x(\lambda)R_y(\theta)C_i, \quad (3)$$

to each atomic position ( $C_i$ ), where  $R_x(\lambda)$ ,  $R_y(\theta)$ , and  $R_z(\kappa)$  represent counterclockwise rotations about the  $x$ ,  $y$ , and  $z$  axes, respectively. The angles defining the orientation of each molecule shall be labeled  $\{\lambda_S, \theta_S, \kappa_S\}$  and  $\{\lambda_T, \theta_T, \kappa_T\}$  for the sample- and tip-adsorbed molecules. For investigative purposes, only the  $\lambda_S$  and  $\theta_S$  are needed to define the orientation of the surface-adsorbed molecule, as the third

rotation in  $z$ ,  $\kappa_S$  only has the effect of rotating the final image. As such, this sixth angle is only applied after suitable images are obtained to align with the experimentally observed data, and is not used in the investigative model.

It is also necessary to allow the direction along which the energy lowering functions act,  $\zeta^T$  and  $\zeta^S$ , to vary from the  $Z^T$  axis. This is incorporated via the rotations  $R_x(\chi_T)$  and  $R_y(\nu_T)$  for the tip-adsorbed molecule, and  $R_x(\chi_S)$  and  $R_y(\nu_S)$  for the surface-adsorbed molecule. For the surface-adsorbed molecule, this could represent the effect of the inhomogeneity of the surface, something that is particularly relevant when considering the complicated bonding sites on the Si(111)-(7 × 7) surface. For the tip-adsorbed molecule, the energy-lowering function acts in a line from the tip through the center of the molecule, representing the tilt of the molecule on the tip.

The experimental data have been obtained at positive sample bias, and as such tunneling is expected to occur from the highest occupied molecular orbital (HOMO) of the tip-adsorbed molecule to the lowest unoccupied orbital (LUMO) of the sample-adsorbed molecule. For an isolated  $C_{60}$  molecule, the frontier orbitals consist of a fivefold-degenerate HOMO and a three-fold-degenerate LUMO. The introduction of the bonding interaction reduces these to singlets for all cases except where  $\zeta$  points through a hexagonal face  $\{\nu = \arctan[\phi^2]\}$  [where  $\phi$  is the golden ratio  $\frac{1}{2}(1 + \sqrt{5})\}$ ] or a pentagon face ( $\nu = \arctan[\phi^{-1}]\}$ ). In these cases, the HOMO reduces to two doublets and a singlet, and the LUMO to a doublet and a singlet.<sup>30</sup> Using this method, it is not possible to determine which of these molecular orbitals will be involved in the tunneling process at a given bias, and as such it is necessary to consider each of these possibilities in determining a match with the experimental data.

The simulations undertaken result in images that are, in the overwhelming majority of cases examined, unique, and so it would appear the probability of obtaining a match with experiment that falsely predicts the molecular orientations or MOs is small. Clearly, the parameter space is too large to rule this out completely, although the fast computational time (an investigative image can be produced within a few minutes on a standard desktop computer) allows a large number of parameter values to be investigated.

### III. EXPERIMENTAL METHOD

Experimental STM images obtained with a  $C_{60}$ -functionalized tip of  $C_{60}$  adsorbed on a Si(111)-(7 × 7) surface have been produced using an Omicron Nanotechnology low-temperature STM/AFM system equipped with commercial qPlus sensors (also supplied by Omicron Nanotechnology), as described by Chiu *et al.*<sup>6</sup> The base pressure of the system is typically lower than  $5 \times 10^{-11}$  torr and the microscope temperature was 77 K. Clean Si(111)-(7 × 7) samples were prepared by standard flash annealing, and  $C_{60}$  molecules were deposited onto the surface at room temperature using a simple homemade evaporator comprising a direct current-heated Ta envelope with a small hole in one end (1 mm diameter). The samples were then transferred to the STM head and allowed to cool before imaging.

In order to transfer a molecule from the surface onto the tip, we adopted a number of strategies, including the use of  $I(z)$

spectroscopy directly above an adsorbed  $C_{60}$ . Although  $I(z)$  spectroscopy could be used for the transfer of a single molecule to the tip, we found it much less time consuming to pick up a  $C_{60}$  molecule while imaging in STM mode. We did this by increasing the scan speed, lowering the loop gain, reducing the bias voltage, and increasing the tunnel current. This often leads to the tip “crashing” into the molecule and either translating it across the surface or, not infrequently, picking it up.

Images were taken with an effective positive sample bias, in constant current feedback with an oscillating cantilever [i.e., dynamic STM (dSTM)]. Therefore, our stated tunnel current set-point values represent the average tunnel current over the oscillation cycle; peak tunnel current values (at the point of closest approach) are likely to be significantly higher.

#### IV. RESULTS AND DISCUSSION

To aid in the interpretation of the experimental images, it is beneficial to use any reflectional or rotational symmetry the images possess to approximate the molecular orientation of the two  $C_{60}$ 's and reduce the number of parameters which may be varied. When isolated,  $C_{60}$  is described by the highly symmetric icosahedral point group  $I_h$ , although when an external interaction is present, in this case through bonding with the tip or substrate, it is expected that the molecular distortion that is induced will lower this symmetry. Even so, a number of symmetry operations are expected to be preserved depending on the orientation of the molecule,<sup>26</sup> which are observed in the expected image for certain orientations.

Figure 2 shows possibilities for the STM images obtained for the case where the tip and sample molecules are situated with pentagonal faces aligned with one another [Figs. 2(a)–2(c)], and when the molecules have hexagonal faces aligned [Figs. 2(d)–2(f)]. The relative molecular orientations are

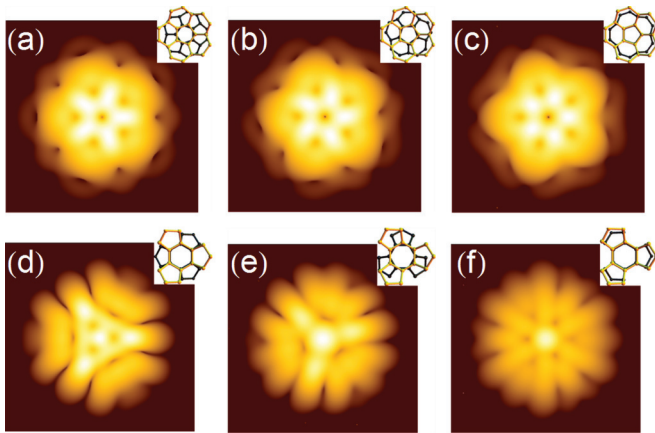


FIG. 2. (Color online) Theoretical STM images for the case where a pentagonal face on each molecule is aligned ( $\theta_T = \theta_S = \arctan[\phi^{-1}]$ ) [(a)  $\kappa_T = 0$ , (b)  $\kappa_T = 2\pi/20$ , (c)  $\kappa_T = 2\pi/10$ ], and two hexagonal faces are aligned ( $\theta_T = \theta_S = \arctan[\phi^2]$ ) [(d)  $\kappa_T = 0$ , (e)  $\kappa_T = 2\pi/12$ , (f)  $\kappa_T = 2\pi/6$ ]. The relative orientations of the two molecules are shown in the inset of each image, with the lighter (yellow online) molecule showing the orientation of the tip-adsorbed molecule, and the black molecule showing the orientation of the surface-adsorbed molecule.

shown in the inset of the theoretical images by looking through the bottom half of the tip-adsorbed molecule (yellow in Fig. 2) onto the upper half of the surface-adsorbed molecule (black in Fig. 2) at the point where the two molecules are exactly aligned during the scan. From the theoretical images, two key features should be noted which are indicative of the higher-symmetry orientations. First, it can be seen in all the images shown that the relevant rotational symmetry is conserved in the images, i.e., Figs. 2(a), 2(b), and 2(c), have  $C_5$  rotational symmetry, and Figs. 2(d), 2(e), and 2(f) have  $C_3$  rotational symmetry. Second, when the reflections in the  $z$  plane are aligned for both molecules [Figs. 2(a), 2(c), 2(d), and 2(f)], this reflection is preserved, and is present in the image obtained.

The results obtained in Fig. 2 are comparable to those obtained by Hauptmann *et al.*<sup>20</sup> where the  $C_{60}$ - $C_{60}$  interaction was modeled by considering orbitals formed from two-dimensional Gaussians which provided a threefold-symmetric pattern for the electron distribution on each hexagonal faces. The comparison between the results here and the experimental and theoretical results obtained by Hauptmann *et al.* is shown in Fig. 3, where it can be seen that by considering both the MO functions as a whole and the split in energy of the MO functions due to the external interactions, a theoretical representation which more closely resembles the experimental images is obtained. In particular, for Fig. 3(i), where the surface molecule is adsorbed with a pentagonal face prone, the local threefold symmetry at the center of the image is more clearly represented. The experimental image shown in Fig. 3(d) also shows evidence of a slight darkening within the triangular feature, that is also observed in the image produced from the method presented here [Fig. 3(j)], but not in the Gaussian approximation [Fig. 3(g)].

It should also be noted that while the match with experiment appears closer using this method, both methods arrive at the same conclusion regarding the relevant orientation of the two molecules, and as such the Gaussian approximation used by Hauptmann *et al.*<sup>20</sup> is clearly a satisfactory approach in this case. However, when looking at interactions between individual molecules, as opposed to the monolayer shown experimentally in Fig. 3, this assumption will only be valid in the central region of the image, as, when the tip is aligned sufficiently off center in relation to the surface-adsorbed molecule, the most significant contribution to the current will no longer be from the uppermost faces. As such, the Gaussian method would need considerable modification to ensure accurate results. To investigate the interaction between two  $C_{60}$  molecules, it is often more desirable to look at single molecules on a surface, as the intermolecular interactions in a monolayer are not present. With this in mind, the remaining experimental work shown here will relate to the case where the interaction with an isolated  $C_{60}$  molecule on a Si(111)-(7 × 7) surface is considered.

While the highly symmetric orientations apply to a limited number of cases, it is still useful to use this symmetry argument to match experimental data. Figure 4(d) shows an experimental image that has (approximately) two planes of reflection perpendicular to each other, as well as an approximate  $C_2$  rotation, indicating that both molecules must be approximately aligned with a double bond facing each other, either with the double bonds aligned or perpendicular to each other. This

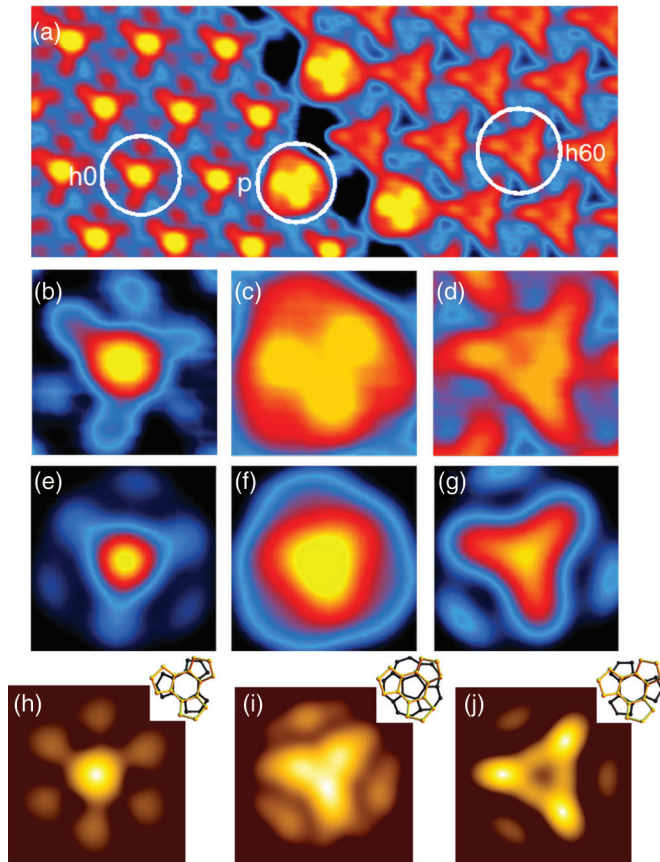


FIG. 3. (Color online) Comparison of experimentally and theoretically obtained images [experiment: (a)–(d), theory: (e)–(g)] (reproduced from Fig. 2 of Hauptmann *et al.* (Ref. 20) Copyright 2012, the Institute of Physics (2012)) and theoretically obtained images using the method presented here [(h)–(j)]. The relevant orientations of the two molecules are shown in the inset of each of the theoretical images obtained from this method (as described in Fig. 2), in close agreement with the orientations postulated by Hauptmann *et al.* The orientation of the tip-adsorbed molecule in (h)–(j) is defined by  $\theta_T = \arctan[\phi^2]$ ,  $\lambda_T = 0$ , and  $\kappa_T = -0.1$ . The surface-adsorbed molecules are defined by (h)  $\theta_T = \arctan[\phi^2]$ ,  $\lambda_S = 0$ ,  $\kappa_S = 0.9$ , (i)  $\theta_T = \arctan[\phi^{-1}]$ ,  $\lambda_S = 0$ ,  $\kappa_S = 0$ , (j)  $\theta_T = \arctan[\phi^2]$ ,  $\lambda_S = 0$ ,  $\kappa_S = 0.1$ .

information can then be used as a starting point to ascertain the molecular orientations of both molecules.

As shown by Herz *et al.*,<sup>7</sup> the structure of the probe determines the appearance of the image formed as a result of the interaction between the adatoms of the Si(111)-(7 × 7) surface and the tip. As such, the MOs involved in the tunneling process for the tip-adsorbed molecule, as well as the molecular orientation of the molecule, may be determined by examining the interaction with the adatoms, using the same reverse imaging technique as shown in Chiutu *et al.*<sup>6</sup> Using the Si(111)-(7 × 7) surface is particularly useful in this case, as the interadatom distance is large, resulting in a more detailed image of the tip from each adatom.

Using this technique, and matching with the experimental data shown in Figs. 4(a) and 4(g), the MOs and orientation of the tip-adsorbed molecule can be found, with the result

that, as anticipated, the molecule is approximately oriented with a double bond facing the surface. The slight tilt on the molecule away from the double bond accounts for the asymmetry of the experimental image where one lobe appears brighter than the other. By matching with the image from the adatoms, the parameters associated with the tip-adsorbed molecule can be fixed. The same parameters can then be used when examining the C<sub>60</sub>-C<sub>60</sub> interaction, assuming that the interaction between the two C<sub>60</sub>'s does not alter the position of the tip-adsorbed molecule. While it is a consideration that the interaction between the two could cause some deviation, there is no experimental evidence that a change in tip state is observed when the surface molecule is scanned, as the image formed between the tip and the adatom does not change after scanning a C<sub>60</sub>. In addition, the theoretical matches provide a good description of the experimentally derived images (as will be shown), and as such it is deduced that any localized “wobbling” as the tip passes over the molecule is small.

With the tip parameters fixed, the orientation and orbitals of the surface molecule can be varied until an appropriate match with the experimental image is found. Using the symmetry of the image, the two double bond prone orientations where the reflectional planes align are first tested, and the different MOs trialed to obtain an image that resembles that found experimentally. From this, it is found that the best match is when the double bonds are aligned, with this orientation then varied to “fine tune” the image until a suitable match is formed, resulting in the theoretical image shown in Fig. 4(c). The MO associated with the sample molecule is shown in Fig. 4(f) to indicate what would be seen during STM if a model-*s*-type tip was used.

In the case shown in Figs. 4(c)–4(f), the symmetry of the image could be used to elucidate the approximate molecular orientations of the two molecules as a starting point for the analysis. However, in general, this will not be the case for most experimentally observed images. Even so, the method can still be used in these more complicated cases, as shown for the second molecule on the experimental image [Fig. 4(h)], where a more “trial-and-error” style approach needs to be taken. Here, the tip-adsorbed molecule will be oriented in the same way as for the previous match, and as such it is only the orientation of the surface molecule, and the MOs associated with it, that need to be varied to obtain the match. The process used to obtain the molecular orientation was to create an initial library of images for the interaction with each MO of the surface-adsorbed molecule, with the molecule oriented with either a hexagon, pentagon, single bond, or atom prone to the surface. In this case, the surface molecule is assumed to not be oriented with a double bond normal to the surface, as this would result in both molecules possessing a C<sub>2</sub> rotation which, as discussed, would be seen in the experimental image. Once these images are produced, it is straightforward to analyze the data to find an image that approximately matches the experimental work, and the various parameters can then be altered until the most suitable match is found. Using this process, a good match with experiment is again found [Fig. 4(i)], with the MO function of the sample molecule shown in Fig. 4(j), and the orientations of the two molecules shown in Fig. 4(k).

For these two matches, the orientations of the surface-adsorbed molecules can be compared with the theoretical

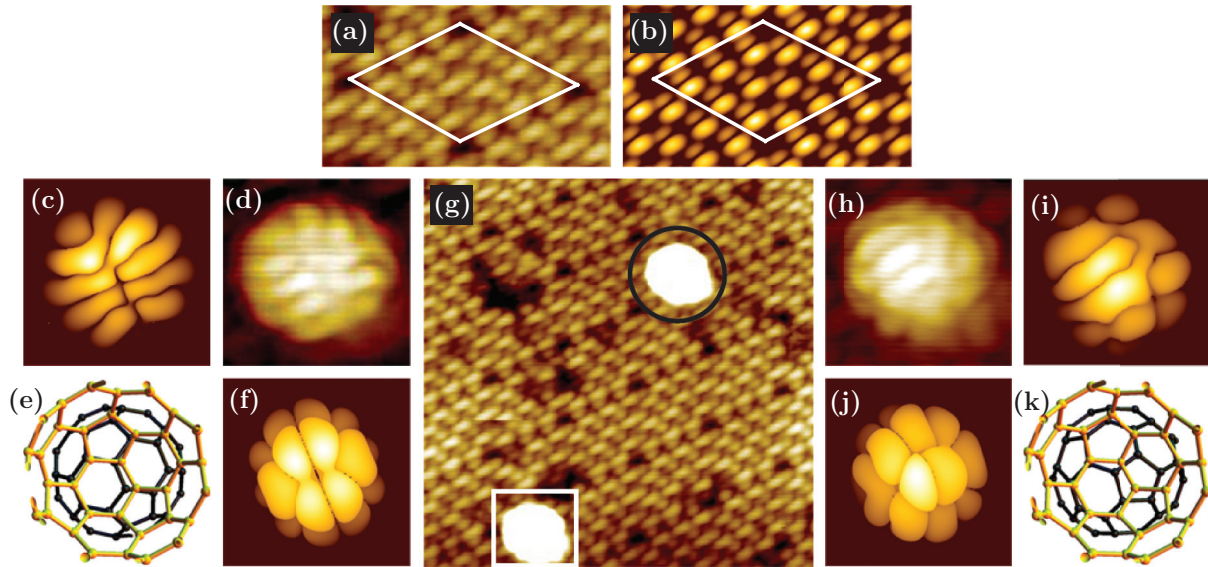


FIG. 4. (Color online) Comparison of theoretical and experimental STM images for a  $C_{60}$ -functionalized tip interacting with the Si(111)- $(7 \times 7)$  surface and two different  $C_{60}$  molecules. (a) The interaction between the tip and surface adatoms taken from the experimental image in (g), and (b) the theoretical interpretation of this ( $\theta_T = -0.1$ ,  $\phi_T = -0.1$ ,  $\kappa_T = 2.1$ ). (c) The theoretical image ( $\theta_S = 0$ ,  $\phi_S = 0$ ,  $\kappa_S = 0.6$ ) to match the experimental image (d) for the interaction between the tip- and surface-adsorbed molecule indicated by the black circle in (g). (e) The relative orientation of the two molecules, (f) the form of the surface-adsorbed MO as if imaged through a model- $s$ -type tip. (h)–(k) The same set of results but for the molecule highlighted by the white square, with (h) experimental image, (i) theoretical match ( $\theta_S = 0.65$ ,  $\phi_S = -0.2$ ,  $\kappa_S = -0.7$ ), the surface molecule as if imaged through an  $s$ -type tip (j), and the relative orientations of the two molecules (k). (Experimental scan parameters:  $V = 2.4$  V,  $\langle I_T \rangle = 500$  pA,  $A_0 = 1.5$  nm).

results obtained by Ruruli *et al.*,<sup>21</sup> where, through the utilization of a tight-binding technique to obtain the most energetically favorable bonding sites, seven stable configurations were postulated for different sites on the Si(111)- $(7 \times 7)$  surface. One of these is the corner-hole (CH) orientation, where the molecule is situated in the gap between six adatoms of the surface structure. The remaining six orientations are all with the  $C_{60}$  situated within a triangle defined by three adatoms, with three different sites ( $C$ ,  $M$ , and  $R$ ) providing two possibilities, each dependent on whether these sites are

on the faulted or unfaulted section of the Si(111)- $(7 \times 7)$  unit cell, represented by the subscripts  $f$  or  $u$ , respectively (full details of these sites are given in Ruruli *et al.*<sup>21</sup>). Analysis of experimental results by Du *et al.*<sup>31</sup> indicates the presence of five of these orientations, namely, the CH,  $M_u$ ,  $M_f$ ,  $C_f$ , and  $C_u$  bonding sites.

A comparison between the bonding sites proposed by Ruruli *et al.*<sup>21</sup> and the results found here is shown in Fig. 5, where excellent agreement is found with two of these bonding sites (the  $R_f$  and  $M_u$  sites). Figure 5(a) corresponds to the

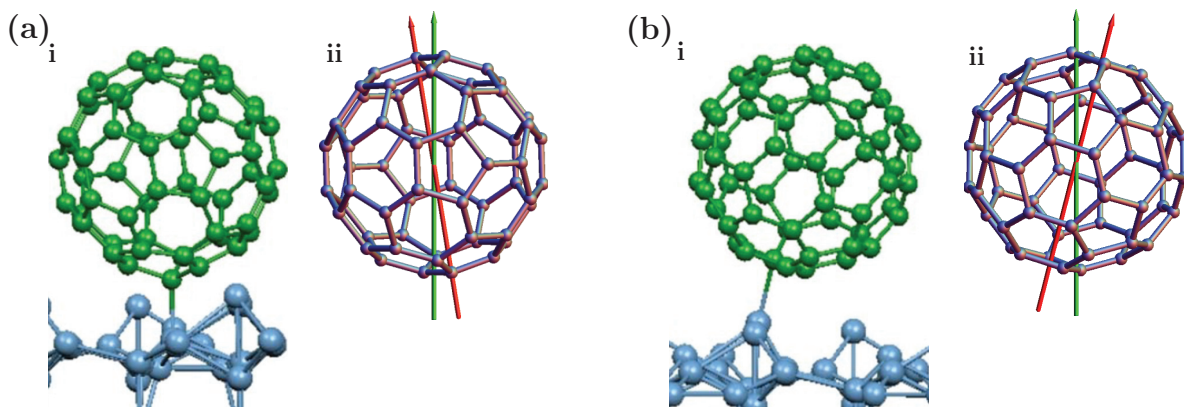


FIG. 5. (Color online) Comparison of the molecular orientations found using the method presented here, and that obtained using a tight-binding technique by Ruruli *et al.* (Ref. 21). (a) (i) Molecular orientation of an  $R_f$  binding site as defined by Ruruli *et al.*, (ii) the orientation of the surface adsorbed molecule from Fig. 4(e) ( $\chi_S = 0$ ,  $\nu_S = -0.05$ ). In (ii) the light arrow (green online) points normal to the surface, and the dark arrow (red online) indicates the direction along which the energy function decays. (b) (i) Molecular orientation for an  $M_u$  binding site, and (ii) for the molecular orientations as found in Fig. 4(k) ( $\chi_S = 0$ ,  $\nu_S = 0.65$ ). Figures (a) (i) and (b) (i) reprinted from Fig. 5 with permission from Ruruli *et al.* (Ref. 21) (Copyright 2010 by the American Physical Society).

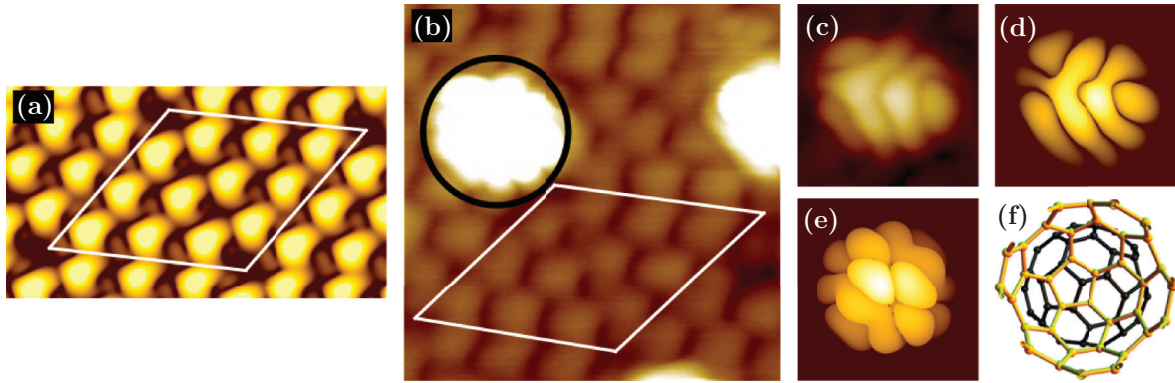


FIG. 6. (Color online) Comparison between experimentally and theoretically obtained STM images. (a) Theoretical simulation for the  $C_{60}$ -adatom interaction as a comparison to the experimental image (b) [Si(111)-(7  $\times$  7) unit cell highlighted in white] ( $\theta_T = 0.75$ ,  $\phi_T = 0$ ,  $\kappa_T = 2.95$ ). (c) Experimental image of the circled molecule, and (d) the theoretical comparison. (e) The sample-adsorbed molecules MO as imaged through an  $s$ -type tip, (f) the relative orientation of the two  $C_{60}$ 's depicted in the same way as in Fig. 2 ( $\theta_S = 0.65$ ,  $\phi_S = -0.2$ ,  $\kappa_S = -1.05$ ). (Experimental scan parameters:  $V = 2.3$  V,  $\langle I_T \rangle = 300$  pA,  $A_0 = 1.5$  nm).

orientation deduced in Fig. 4(e), which shows good agreement with the  $R_f$  bonding site, and Fig. 5(b) shows the molecular orientation from the match in Fig. 4(k), in agreement with the  $M_u$  bonding site. In both cases, the orientation deduced by Rurali *et al.* is shown in (i), and the orientation found from the method shown here in (ii). The agreement is particularly close for the  $M_u$  bonding site in Fig. 5(b), where the axis depicting the energy-reducing function aligns closely with the Si-C bond.

In making this comparison, it is important to consider the errors associated with the orientational parameters of the molecules. It is difficult to quantify this error, as a suitable match is obtained by eye as opposed to a specific quantitative process. Also, the different parameters have a varying effect on the image, and as such the error of each is different. Even so, our simulations indicate that the orientations postulated for the examples in this work are accurate to within around  $\pm 3^\circ$  in any direction. While a number of theoretical images have been obtained for various other orientations, the large parameter space makes it impractical to assign a general error value for the technique. The error would need to be ascertained separately for each case considered, although the images obtained for the cases considered in this paper and the other orientations we have considered suggest that the error is likely to be around the  $\pm 3^\circ$  value.

The results obtained here correlate well with some of the orientations postulated in Rurali *et al.*<sup>21</sup> and, as such, to further reduce the complexity of this particular system it can be beneficial to use these orientations as starting points for the molecular orientations of the surface-adsorbed molecules. One such case is shown in Fig. 6, where the surface-adsorbed molecule is in the  $M_u$  configuration. Again, the interaction with the tip-adsorbed molecule and the adatoms on the surface can be used to elucidate the tip configuration. In this case, the interaction with the adatom provides the match shown in Fig. 6(a) where the molecule is situated with a single bond approximately facing the surface. Taking this orientation and the MO function, along with the orientation predicted for the surface molecule for the  $M_u$  bonding site, the result shown in Fig. 6(d) is obtained, where again excellent

agreement is found with the experimental data [shown in Fig. 6(c)].

## V. CONCLUSIONS

From the experimental data presented here, the molecular orientations of two interacting  $C_{60}$  molecules have been elucidated along with the MO functions involved in the tunneling process. The orientations deduced have been compared with previous theoretical calculations on the optimum bonding sites on the Si(111)-(7  $\times$  7) surface undertaken by Rurali *et al.*,<sup>21</sup> showing excellent agreement with the  $M_u$  and  $R_f$  bonding sites. That the orientations match with previous theoretical work, and excellent agreement is found between the theoretical images and the experimental images for both the  $C_{60}$ - $C_{60}$  interaction, and the interaction with the Si(111)-(7  $\times$  7) surface, illustrates the validity of the technique.

The method presented allows theoretical images to be constructed on a time scale of around one or two minutes on a standard desktop computer, allowing for speedy analysis of the experimental images. While this work has utilized standard Hückel theory to obtain the MOs, the method would be equally applicable to any system where the MOs of both tip and sample are constructed using a different LCAO technique. This linear combination allows the the integral associated with Bardeen's tunneling matrix element,<sup>22</sup> from which the derivative rule is derived, to be separable into individual contributions from each atomic orbital. This allows the use of the atomic "derivative rule"<sup>23</sup> for each separate atomic orbital to obtain the current for interacting MOs at any given point in the form of a summation of derivatives. This negates the need to compute any integrals, as would usually be the case when examining tip-sample convolution, saving considerable computational time.

By using the symmetry of the experimental images it has been shown that in certain cases, estimations of the molecular orientations can be obtained via a systematic approach, which can then be used as a starting point to reduce the time needed to interpret the experimental images. It is clear that from using the ideas presented here as a basis, it would be possible to investigate other properties, such as the intermolecular force,

or conductance of the two molecules, that may be dependent on the orientation of the two  $C_{60}$ 's, as well as providing important parameters which could be used alongside more computationally expensive techniques such as DFT to obtain further information on the system. Additionally, and somewhat surprisingly, the simplistic way in which the bonding interaction between the  $C_{60}$  and the Si(111)-(7 × 7) surface has been incorporated has produced excellent agreement with experiment. That the method is successful at interpreting images from this complex surface shows the generality of the technique for considering simpler surfaces such as the commonly used Cu(111) or Au(111) structures.

## ACKNOWLEDGMENTS

P.M. and A.M.S. acknowledge the Engineering and Physical Sciences Research Council (EPSRC) and the Leverhulme Trust, respectively, for funding via Grants No. EP/G007837/1 and No. F00/114 BI. A.J.L. is funded through an EPSRC doctoral training account, and C.C. is grateful for a Marie Curie fellowship funded by the NANOCAGE FP6 training network. We also acknowledge funding from the European Commission's ICT-FET programme via the Atomic Scale and Single Molecule Logic Gate Technologies (AtMol) project, Contract No. 270028.

\*janette.dunn@nottingham.ac.uk

- <sup>1</sup>L. Gross, F. Mohn, N. Moll, P. Liljeroth, and G. Meyer, *Science* **325**, 1110 (2009).
- <sup>2</sup>L. Gross, *Nat. Chem.* **3**, 493 (2011).
- <sup>3</sup>M. Nicklaus, A. Pignolet, C. Harnagea, and A. Ruediger, *Appl. Phys. Lett.* **98**, 162901 (2011).
- <sup>4</sup>L. Gross, F. Mohn, N. Moll, G. Meyer, R. Ebel, W. M. Abdel-Mageed, and M. Jaspars, *Nat. Chem.* **2**, 821 (2010).
- <sup>5</sup>Z. X. Sun, M. P. Boneschanscher, I. Swart, D. Vanmaekelbergh, and P. Liljeroth, *Phys. Rev. Lett.* **106**, 046104 (2011).
- <sup>6</sup>C. Chiutu, A. M. Sweetman, A. J. Lakin, A. Stannard, S. Jarvis, L. Kantorovich, J. L. Dunn, and P. Moriarty, *Phys. Rev. Lett.* **109**, 079901(E) (2012).
- <sup>7</sup>M. Herz, F. J. Giessibl, and J. Mannhart, *Phys. Rev. B* **68**, 045301 (2003).
- <sup>8</sup>L. Gross, N. Moll, F. Mohn, A. Curioni, G. Meyer, F. Hanke, and M. Persson, *Phys. Rev. Lett.* **107**, 086101 (2011).
- <sup>9</sup>G. Schull, T. Frederiksen, M. Brandbyge, and R. Berndt, *Phys. Rev. Lett.* **103**, 206803 (2009).
- <sup>10</sup>G. Schull, T. Frederiksen, A. Arnau, D. Sanchez-Portal, and R. Berndt, *Nat. Nanotechnol.* **6**, 23 (2011).
- <sup>11</sup>A. N. Chaika and A. N. Myagkov, *Chem. Phys. Lett.* **453**, 217 (2008).
- <sup>12</sup>A. N. Chaika, V. N. Semenov, V. G. Glebovskiy, and S. I. Bozhko, *Appl. Phys. Lett.* **95**, 173107 (2009).
- <sup>13</sup>A. N. Chaika, S. S. Nazin, V. N. Semenov, S. I. Bozhko, O. Lubben, S. A. Krasnikov, K. Radican, and I. V. Shvets, *Europhys. Lett.* **92**, 46003 (2010).
- <sup>14</sup>A. N. Chaika, S. S. Nazin, V. N. Semenov, N. N. Orlova, S. I. Bozhko, O. Lubben, S. A. Krasnikov, K. Radican, and I. V. Shvets, *Appl. Surf. Sci.* **267**, 219 (2013).
- <sup>15</sup>J. Loos, *Adv. Mater.* **17**, 1821 (2005).
- <sup>16</sup>J. H. A. Hagelaar, C. F. J. Flipse, and J. I. Cerda, *Phys. Rev. B* **78**, 161405 (2008).
- <sup>17</sup>A. D. Gottlieb and L. Wesoloski, *Nanotechnology* **17**, R57 (2006).
- <sup>18</sup>C. Weiss, C. Wagner, C. Kleimann, M. Rohlfing, F. S. Tautz, and R. Temirov, *Phys. Rev. Lett.* **105**, 086103 (2010).
- <sup>19</sup>M. Švec, P. Merino, Y. J. Dappe, C. González, E. Abad, P. Jelínek, and J. A. Martín-Gago, *Phys. Rev. B* **86**, 121407 (2012).
- <sup>20</sup>N. Hauptmann, F. Mohn, L. Gross, G. Meyer, T. Frederiksen, and R. Berndt, *New J. Phys.* **14**, 073032 (2012).
- <sup>21</sup>R. Rurali, R. Cuadrado, and J. I. Cerda, *Phys. Rev. B* **81**, 075419 (2010).
- <sup>22</sup>J. Bardeen, *Phys. Rev. Lett.* **6**, 57 (1961).
- <sup>23</sup>C. J. Chen, *Phys. Rev. B* **42**, 8841 (1990).
- <sup>24</sup>J. Tersoff and D. R. Hamann, *Phys. Rev. B* **31**, 805 (1985).
- <sup>25</sup>J. I. Pascual, J. Gomez-Herrero, C. Rogero, A. M. Baro, D. Sanchez-Portal, E. Artacho, P. Ordejon, and J. M. Soler, *Chem. Phys. Lett.* **321**, 78 (2000).
- <sup>26</sup>J. L. Dunn, A. J. Lakin, and I. D. Hands, *New J. Phys.* **14**, 083038 (2012).
- <sup>27</sup>M. Menon, E. Richter, and K. R. Subbaswamy, *J. Chem. Phys.* **104**, 5875 (1996).
- <sup>28</sup>Y. F. Deng and C. N. Yang, *Phys. Lett. A* **170**, 116 (1992).
- <sup>29</sup>I. D. Hands, J. L. Dunn, and C. A. Bates, *Phys. Rev. B* **81**, 205440 (2010).
- <sup>30</sup>B. W. Heinrich, M. V. Rastei, D. J. Choi, T. Frederiksen, and L. Limot, *Phys. Rev. Lett.* **107**, 246801 (2011).
- <sup>31</sup>X. L. Du, F. Chen, X. Chen, X. X. Wu, Y. X. Cai, X. Q. Liu, and L. Wang, *Appl. Phys. Lett.* **97**, 253106 (2010).